

as the hydrogen pressure was varied in the rollover regime also permitted the deduction of the stoichiometries of the adsorbed product hydrocarbon fragments. The hydrogenolysis of *n*-butane on the Ir(110)-(1×2) surface could not be described by the mechanism involving irreversible C-C bond cleavage. Rather, a mechanism involving reversible C-C bond cleavage in a symmetrical reaction intermediate was found to provide a superior fit to the data.

Ethane hydrogenolysis was determined to proceed through different reaction intermediates, the parent fragment on the Ir(110)-(1×2) surface being more extensively dehydrogenated. We interpreted this result as a manifestation of the availability of high-coordination adsites on the (110)-(1×2) surface. Both propane and neopentane hydrogenolysis were found to be nearly indistinguishable on the two surfaces. These results can be interpreted by invoking reaction intermediates that are bound to two or more adjacent metal surface atoms. However, the participation of a mononuclear metallacycle butane in the hydrogenolysis of propane remains a distinct possibility. Comparing the specific rates of hydrogenolysis (to methane and ethane) of propane and cyclopropane¹⁸ on the Ir(110)-(1×2) surface, we have lent considerable support to our assignment of the apparent activation energy to $E_{app} \approx E_C + \Delta H^\ddagger$ for temperatures below rollover and $E_{app} \approx E_C$ for temperatures above rollover.

The selectivity for the hydrogenolysis of *n*-butane on the two surfaces has been identified with the occurrence of particular, adsorbed reaction intermediates on each surface. When our results are compared to those reported previously on supported iridium catalysts of varying metallic particle size,²² a direct correlation

has been discovered between the selectivity for ethane production and the concentration of low coordination number metal surface atoms.⁴⁹ On the basis of the implicated reaction mechanism and precedents from organometallic chemistry,⁶² the adsorbed reaction intermediate that leads to the high selectivity for ethane is a mononuclear metallacycle pentane, the formation of which is sterically forbidden on the (111) surface. The logical extension of this observation has led us to propose that other mechanisms involving, for example, mononuclear metallacycle hexanes⁶⁷ may also be forbidden on (111) surfaces. On the other hand, the observed reversibility of the metallacycle pentane-bis(ethylene) interconversion has led us to propose that these metallacycle pentane intermediates may be involved in the isomerization of higher hydrocarbons such as branched butanes and pentanes, particularly on highly dispersed catalysts.

Acknowledgment. This work was performed at Sandia National Laboratories and supported by the U.S. Department of Energy under Contract DE-AC04-76DP00789. We acknowledge the partial support of the Office of Basic Energy Sciences, Division of Chemical Science (D.W.G.), and National Science Foundation Grant No. DMR-8500789 (W.H.W.).

Registry No. C₂H₆, 74-84-0; C₃H₈, 74-98-6; C₄H₁₀, 106-97-8; *neo*-C₅H₁₂, 463-82-1; Ir, 7439-88-5.

Supplementary Material Available: Details of mechanistic modeling of the hydrogenolysis of alkanes on iridium and the microscopic significance of kinetic parameters (11 pages). Ordering information is given on any current masthead page.

Matrix Isolation Infrared Studies of Nucleic Acid Constituents. 5.[†] Experimental Matrix-Isolation and Theoretical *ab Initio* SCF Molecular Orbital Studies of the Infrared Spectra of Cytosine Monomers

M. Szczesniak,[‡] K. Szczepaniak, J. S. Kwiatkowski,[§] K. KuBulat, and W. B. Person*

Contribution from the Department of Chemistry, University of Florida, Gainesville, Florida 32611. Received March 21, 1988

Abstract: Results are presented from an experimental study of the infrared spectra of cytosine and its deuterated derivatives isolated in an inert Ar matrix and also in an N₂ matrix deposited on a window at 15 K. These spectra show that isolated cytosine exists under these conditions as a mixture of the "normal" amino-oxo (a-o) tautomer and the "rare" amino-hydroxy (a-h) tautomer; in fact, the last form predominates in both matrices with an "equilibrium constant" $K_i(o/h) = [a-o]/[a-h]$ measured to be about 0.5. Infrared spectra of the crystalline solid are also presented, and they agree with the conclusion from X-ray diffraction studies that only the normal amino-oxo tautomer occurs in the solid. In order to interpret the observed infrared spectra, we have carried out an *ab initio* molecular orbital calculation of the spectra of both tautomers at the SCF level with a 3-21G basis set. The calculation predicts frequencies, absolute infrared intensities, and potential energy distributions (PEDs) for all normal modes of each tautomer to provide a basis for the assignment of the experimental spectra. The latter problem was aided greatly by the discovery that irradiation of cytosine isolated in an Ar matrix with UV light changes the relative concentrations of the two tautomers in the matrix. Application of this technique in our studies allowed us to separate the absorption spectra to obtain the complete infrared spectrum for each tautomer free from the absorption by the other form. Each separate spectrum was thus assigned with a reasonable degree of confidence by comparison with the calculated spectra. The relatively good agreement between calculated and experimental spectra for each tautomer provides support for confidence in the validity of the use of these calculated vibrational parameters as a basis for predicting spectra of cytosine and its derivatives. Finally, the effect of intermolecular interaction upon the spectrum of cytosine is examined in a comparison of the spectra of matrix-isolated samples with the spectrum of the crystalline solid.

Vibrational spectra of cytosine and of its corresponding nucleoside and nucleotide, as well as of several of its derivatives, have been the subject of numerous experimental studies in solution and

in the solid phase (ref 1 and references given therein). These studies establish the predominance of the amino-oxo form for the cytosine residue, which is the same form as is considered to be involved in the base-pairing scheme in DNA.

Although studies of the vibrational spectra of nucleic acid bases such as cytosine in the solid state or dissolved in polar solutions

[†] Part 4 of this series is ref 23.

[‡] On leave (1986-1988) from the Institute of Physics, Polish Academy of Sciences, 02-668 Warsaw, Poland.

[§] On leave (1985-1986) from the Institute of Physics, N. Copernicus University, 87-100 Torun, Poland.

(1) Kwiatkowski, J. S.; Pullman, B. *Adv. Heterocycl. Chem.* **1975**, *18*, 199.

the reader is referred to our previous papers.^{27,28} For a general review of the predictions of stabilities of tautomeric forms of molecules, including cytosine, by quantum mechanical methods, see ref 38. Here, we state that calculations with small basis sets predict the a-o form to be more stable than the a-h form, but, as the quality of the basis set improves and as correlation effects are considered, the energy calculated for the a-h form becomes lower and lower until it is estimated at the highest level of calculation (with the zero-point vibrational correction) to be lower in energy than the a-o form by about 1 kJ/mol, in agreement with our experimental findings given below.

It is worthwhile to note that the prediction of the vibrational spectrum of the a-o tautomer of cytosine has been a subject of several theoretical studies including an ab initio SCF-MO calculation,³⁹ force refinement formalism,⁴⁰⁻⁴¹ and a molecular mechanics force field.⁴² Normal-coordinate calculations were performed also for 5-methylcytosine with a simple Urey-Bradley force field for the in-plane vibrations and a valence force field for the out-of-plane vibrations of the planar skeleton⁴³ and with a semiempirical force field.^{15b} Very recently, a semiempirical calculation using the CNDO/2 method has been performed to predict the vibrational spectra of cytosine,²⁶ 1-methylcytosine,⁴⁴ and 5-fluorocytosine.⁴⁵

Methods

A. Experimental Procedure. The infrared spectra were studied with a Nicolet Model 7199 FTIR spectrometer at a resolution of 1 cm⁻¹. The matrix sample was formed by deposition of cytosine vapor together with a matrix gas (in large excess) onto a CsI window attached to the cold finger of a closed-cycle He cryostat (Displex CSA 202E) cooled to about 15 K. The solid sample was evaporated at a temperature of about 220 °C from a small electrically heated glass furnace located in a chamber attached to the lower part of the cryostat. The temperature of the furnace was measured by a chromel/constantan thermocouple fastened to the external surface of the furnace. The matrix gas was introduced through a separate inlet placed in the vicinity of the furnace. A flow (at rate of several millimole/hour) of matrix gas was initiated prior to turning on the furnace heater and continued until the heater had returned to room temperature. The matrix gas was passed through a precooled liquid-N₂ trap located between the matrix-gas container and the cryostat and condensed on the cold CsI window. The temperature of the cold finger of the cryostat was measured with a chromel/gold (iron doped) thermocouple attached to the copper frame of the cold window. The pressure inside the cryostat prior to deposition, with the cold finger at its lowest temperature, was about 5 × 10⁻⁷ Torr. During deposition the cryostat was still evacuated with the pressure kept at about 5 × 10⁻⁶ Torr. The time required to deposit a sample sufficient for spectroscopic investigation was about 10 h. The amount of the sample deposited was controlled by monitoring the spectrum during deposition. The sample of cytosine (and of *D*-cytosine) was purified by the vacuum sublimation occurring during the deposition process. To prove that the compound did not decompose during heating to form the matrix sample, we have compared the spectrum of an annealed solid film, formed by evaporation of cytosine at the same furnace temperature as for matrix study, with that of a cytosine sample in a KBr pellet. The spectra from both samples were found to be identical.

The UV irradiation of a matrix sample was performed with a 100-W Xenon lamp. The irradiation was done either through both the quartz outside window and the CsI window (working as a filter), transmitting UV light down to 250 nm, or without the CsI window but through the quartz window, transmitting UV light down to 200 nm. Irradiation through the CsI-quartz window pair causes a gradual decrease of the absorbance of the bands related to the a-o tautomer (e.g., the N₁H

stretch) relative to the absorbance of the bands corresponding to the a-h tautomer (e.g., the OH stretch). Irradiation through the quartz window only causes a gradual decrease of absorption bands for both tautomers.

Cytosine was purchased from Sigma. *D*-Cytosine was obtained by repeated (seven times) recrystallization from a D₂O solution maintained at ambient temperature. Matrix gases (Ar and N₂) of Matheson Research Purity were used.

B. Computational Details. The numerical calculations were carried out at the Hartree-Fock level with the Pople split-valence shell 3-21G basis set.⁴⁷ Geometry optimization has been performed with the GAUSSIAN 82 program⁴⁸ under the constraint that the cytosine tautomers are planar. This assumption of planarity of the tautomers in question deserves some comment, because it may not be correct. Molecules with amino groups are found, in general, to be nonplanar; this is also the case for amino tautomers of cytosine.⁴⁹⁻⁵² However, the deviations from nonplanarity for the systems under study are small (compare the discussion given for the structure of the oxo tautomer of cytosine⁵⁰), and consideration of nonplanarity would not significantly change the conclusions regarding the vibrational spectrum.

The geometries of both tautomers have been previously optimized by Scanlan and Hillier⁵³ using a 3-21G basis set. Since they used a slightly softer gradient condition for optimization than is used for the GAUSSIAN 82 program, we reoptimized once again the geometries of the tautomers using the geometries from ref 53 as a starting point. These calculated equilibrium structures for the tautomers used for the normal-coordinate calculations are shown in the supplementary material.

The force constant matrices F_x for the in-plane and out-of-plane Cartesian displacements were obtained by numerical differentiation (with displacements of each atom in each direction by ±0.005 Å) of the analytical gradient at the equilibrium geometries. The normal-coordinate transformation matrix l and vibrational frequencies were calculated by diagonalizing the resulting force constant matrix F_q in mass-weighted Cartesian coordinates. Transformation of F_x to the force constant matrix in internal symmetry coordinates for in-plane vibrations and for out-of-plane vibrations (nonredundant symmetry coordinates were defined as recommended by Pulay et al.^{54,55}) and allowed ordinary normal-coordinate calculations to be carried out as described by Schachtschneider.⁵⁶

The calculated frequencies of all normal modes were scaled by multiplication by a single factor of 0.91, which brings the calculated and experimental frequencies of the most reliably assigned N₁H, NH₂, and OH stretches into almost perfect agreement but leads to slightly worse agreement for the lower frequency modes. We did not use different scaling factors for different modes, as many authors do (e.g. in ref 57 and 58) in order to avoid misinterpretation of the bands in frequency region below 1700 cm⁻¹. We believe that we may be able to refine the scaling factors further to use different factors for different normal modes, after accumulating and analyzing results from our other ab initio calculations and experimental matrix studies for a large number of pyrimidine and purine bases. At present, even with a single scaling factor 0.91, the average discrepancy between calculated (scaled) and experimental frequencies is not larger than 3%, even when the out-of-plane modes are included. The discrepancy for these latter modes is known to be much larger. For many of the in-plane modes the discrepancy between calculated (scaled) and experimental frequencies is less than 1%.

Vibrational intensities have been obtained from calculated atomic polar tensors (APT).⁵⁹ Since the force constants have been calculated by numerical differentiation to obtain the energy gradient, the numerical

(47) Binkley, J. S.; Pople, J. A.; Hehre, W. J. *J. Am. Chem. Soc.* **1980**, *102*, 939.

(48) Binkley, J. S.; Frisch, M. J.; DeFrees, D. J. E.; Raghavachari, K.; Whiteside, R. S.; Schlegel, H. B.; Fluder, E. M.; Pople, J. A. *Gaussian 82*; Carnegie-Mellon University: Pittsburgh, PA, 1982.

(49) Kwiatkowski, J. S.; Lesyng, B.; Palmer, M. H.; Saenger, W. Z. *Naturforsch., C: Biosci.* **1982**, *37C*, 937.

(50) Palmer, M. H.; Wheeler, J. R.; Kwiatkowski, J. S.; Lesyng, B. *THEOCHEM* **1983**, *92*, 283.

(51) Boggs, J. E.; Niu, Z. J. *J. Comput. Chem.* **1985**, *6*, 46.

(52) Sygula, A.; Buda, A. *THEOCHEM* **1985**, *121*, 133.

(53) Scanlan, M. J.; Hillier, I. H. *J. Am. Chem. Soc.* **1984**, *106*, 3737.

(54) Pulay, P.; Fogarasi, G.; Pang, F.; Boggs, J. E. *J. Am. Chem. Soc.* **1979**, *101*, 2550.

(55) Fogarasi, G.; Pulay, P. In *Vibrational Spectra and Structure*; Durig, J. R., Ed.; Elsevier: Amsterdam, The Netherlands, 1985; Vol. 14, p 125.

(56) Schachtschneider, H. J. Technical Report, Shell Development Co.: Emeryville, CA, 1969.

(57) Harsanyi, L.; Csaszar, P.; Boggs, J. E. *Int. J. Quantum Chem.* **1986**, *29*, 799.

(58) Fan, K.; Boggs, J. E. *J. Mol. Struct.* **1986**, *32*, 283.

(59) Person, W. B. In *Vibrational Intensities in Infrared and Raman Spectroscopy*; Person, W. B., Zerbi, G., Eds.; Elsevier: Amsterdam, The Netherlands, 1982; Chapters 4 and 14, and references given there.

(38) Kwiatkowski, J. S.; Zielinski, T. J.; Rein, R. *Adv. Quantum Chem.* **1986**, *18*, 85.

(39) Nishimura, Y.; Tsuboi, M. *Chem. Phys.* **1985**, *98*, 71.

(40) Putnam, B. F.; Van Zandt, L. L. *J. Comput. Chem.* **1982**, *3*, 297.

(41) Putnam, B. F.; Van Zandt, L. L. *J. Comput. Chem.* **1982**, *3*, 305.

(42) Weiner, S. J.; Kollman, P. J.; Nguyen, D. T.; Case, D. A. *J. Comput. Chem.* **1986**, *7*, 230.

(43) Aruna, S.; Shanmugan, G. *J. Raman Spectrosc.* **1985**, *16*, 229.

(44) Kuczera, K.; Szczesniak, M.; Szczepaniak, K. *J. Mol. Struct.* **1988**, *172*, 73.

(45) Kuczera, K.; Szczesniak, M.; Szczepaniak, K. *J. Mol. Struct.* **1988**, *172*, 89.

(46) Nowak, M. J. XVllth European Congress on Molecular Spectroscopy, Amsterdam, 1987; Abstracts, p 129.

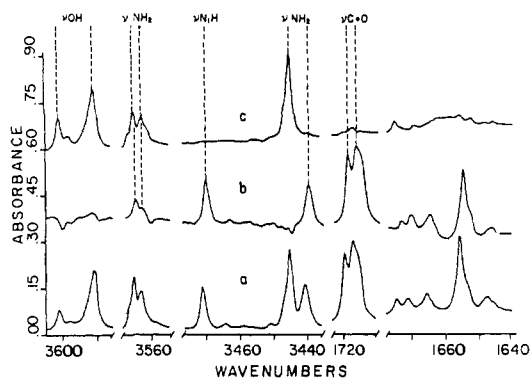


Figure 1. Infrared spectrum in the OH, NH, and C=O stretching region of cytosine isolated in an argon matrix at 15 K: (a) Initial spectrum after matrix deposition and before UV irradiation, with absorption from all tautomers of cytosine. (b) Spectrum of the amino-oxo tautomer obtained as a result of subtraction from the initial spectrum of the spectrum after UV irradiation with the absorbances multiplied by a factor 1.2 to account for a small decrease of the absorbance of all bands due to UV irradiation of the matrix. (c) Spectrum of the amino-hydroxy tautomer obtained as a result of UV irradiation of the matrix sample. The traces of the amino-oxo tautomer remaining after the irradiation were removed from this spectrum by subtraction of the initial spectrum (with the absorbances multiplied by a factor 0.25) from the spectrum after UV irradiation.

dipole moment derivatives (APTs) could also be calculated simultaneously. It is worth noting, however, that the APTs can easily be calculated from separate calculations with the method of Komornicki and McIver.⁶⁰ This type of calculation is particularly useful (a) when the force constants are calculated analytically or (b) when a better basis set (e.g., a basis set augmented with diffuse and polarization functions) is required to calculate the vibrational intensities (or APTs) than is used to calculate the force constants. We have used the method of Komornicki and McIver⁶⁰ to calculate the APTs. In the supplementary material, we present equilibrium geometries, the definition of symmetry coordinates, diagonal elements of force constants matrix, and the APTs calculated for both tautomers with the method of Komornicki and McIver.⁶⁰

Results and Discussion

The examination of the spectral results will be divided into three parts. In the first part, the presence of two tautomers of cytosine in Ar and N₂ matrices is established and the value of the equilibrium constant is determined. In the second part, the complete assignment of all absorption bands observed in the spectrum to the normal modes of vibration for the a-o and the a-h tautomers of cytosine is proposed. In the third part, the effect of intermolecular interactions on the tautomeric equilibrium and on the IR spectra is examined.

1. Tautomeric Equilibrium of Cytosine Molecules Isolated in an Inert Matrix. To establish the tautomeric equilibrium of cytosine that exists in an inert matrix, we begin our discussion of the spectra with the analysis of the C=O, NH, and OH stretching region. These absorption bands give the most straightforward information about the tautomeric forms present, because they correspond to the characteristic, well-localized vibrations of the functional groups directly involved in tautomeric changes. Figure 1 shows this spectral region for cytosine in an Ar matrix.

Only three modes are expected in the OH, NH stretching region if only one a-o tautomer is present: namely, the N1H stretching mode, the asymmetric NH₂ stretching mode, the symmetric NH₂ stretching mode, and the strong C=O stretch near 1700 cm⁻¹. In contrast to this simple expectation, a much more complex spectrum is observed (Figure 1).

Irradiation of the matrix sample by UV light drastically changes this spectrum (Figure 1c). Namely, the absorbance of the bands near 3565, 3471, 3441, 1720, and 1650 cm⁻¹ strongly decreases while the absorbance of the other bands in this region remains

almost unchanged. The most characteristic feature of the spectrum obtained after UV irradiation (Figure 1c) is almost complete disappearance of the absorption near 1720 cm⁻¹ related to the C=O stretch. The absence of the C=O stretching absorption proves that the molecules responsible for the spectrum shown in Figure 1b are those in the a-h tautomeric form. This conclusion is consistent with the appearance of the absorption at 3591 cm⁻¹, where the ν(OH) stretch has been observed for a number of hydroxypyrimidines isolated in low-temperature matrices.^{11,12} The other bands observed in the spectrum in Figure 1c have frequencies very close to those observed for the NH₂ stretching bands of matrix-isolated 5-fluorocytosine, which, in an inert matrix, adopts only the amino-hydroxy form.⁴⁵

The IR spectra of the molecules that are strongly affected by the UV irradiation of the matrix sample can be obtained by subtraction of the spectrum after UV irradiation from the initial spectrum. Such subtraction leads to the cancellation of all bands that are not significantly affected by the UV irradiation. This difference spectrum (Figure 1b) shows a strong C=O stretching absorption near 1700 cm⁻¹, which proves that the strongly affected molecules responsible for the spectrum (Figure 1c) are the oxo tautomers. This conclusion is confirmed by the appearance in this spectrum of the characteristic N1H stretch at 3471 cm⁻¹, close to the frequency observed for the corresponding NH stretch of matrix-isolated 1-methyluracil and uracil.^{19,20,24} The other bands observed in this spectrum (Figure 1b) are related to the asymmetric and symmetric stretching vibrations of the NH₂ group. They have frequencies close to those observed for matrix-isolated 1-methylcytosine, which exists in the matrix in the amino-oxo form.⁴⁴

The ratio of the integrated absorbances (e.g. $a(\text{OH}) = \int \log(I_0/I) dv$) for the OH and N1H stretching modes is proportional to the hydroxy-oxo equilibrium constant with a proportionality factor equal to the ratio of the integrated molar absorption coefficients (A) for these vibrations:

$$K_1 = [a\text{-o}]/[a\text{-h}] = K_1(o/h) = \frac{[a(\text{NH})/a(\text{OH})][A(\text{OH})/A(\text{NH})]}{[A(\text{OH})/A(\text{NH})]}$$

The ratio of $a(\text{NH})/a(\text{OH})$ obtained from the experimental matrix spectrum is 0.35 for cytosine in an Ar matrix and 0.32 for cytosine in an N₂ matrix. Since the ratio of integrated molar absorption coefficients $A(\text{OH})/A(\text{NH})$ can not be obtained from experiment, we shall use the calculated ratio of intensities. These values are $A(\text{NH}) = 105 \text{ km/mol}^{-1}$ and $A(\text{OH}) = 119 \text{ km/mol}^{-1}$ (see Table I), leading to a ratio $A(\text{OH})/A(\text{NH}) = 1.14$, so that $K_1(o/h) = 0.40$ for Ar and $K_1(o/h) = 0.36$ for the N₂ matrix.

The value of $K(o/h)$ can also be estimated from the stretching vibrations of the NH₂ group. It is known that the asymmetric stretching vibration usually appears near 3560 cm⁻¹ and the symmetric stretching is usually near 3440 cm⁻¹ with the ratio of absorbances $a_{as}(\text{NH}_2)/a_s(\text{NH}_2)$ varying between 0.7 and 0.6.^{13,15,23,25,61-64} In the spectrum of cytosine in the argon matrix shown in Figure 1, both these characteristic absorption bands are clearly present. The absorption near 3440 cm⁻¹ due to the symmetric NH₂ stretch consists of two well-resolved components with maxima at 3445 and 3441 cm⁻¹, corresponding to the a-h and a-o tautomers, respectively (see the spectrum after subtraction shown in Figure 1b and 1c). From the ratio of the integrated absorbances for each of the split components observed for the symmetric NH₂ stretch, the value of $K_1(o/h)$ can be estimated. Under the assumption that the integrated molar absorption coefficients for ν_s(NH₂) is the same in both forms, which is in agreement with predictions from our calculation (see Table I), this estimation leads to a value for the $K_1(o/h)$ of 0.54 in the Ar matrix and 0.59 in the N₂ matrix, close to the values previously obtained from the ratio of N1H and OH stretching absorbances.

(61) Purnell, C. J.; Barnes, A. J.; Suzuki, S.; Ball, D. F.; Orville-Thomas, W. *J. Chem. Phys.* **1976**, *12*, 77.

(62) Evans, J. C. *Spectrochim. Acta* **1960**, *16*, 428.

(63) Räsänen, M. *J. Mol. Struct.* **1983**, *101*, 275.

(64) Brown, D. J.; Hoerger, E.; Mason, S. F. *J. Chem. Soc.* **1955**, 4035.

(60) (a) Komornicki, A.; McIver, J. W. *J. Chem. Phys.* **1979**, *70*, 2014.
(b) Schaad, L. J.; Ewig, C. S.; Hess, B. A., Jr.; Michalska, D. *J. Chem. Phys.* **1985**, *83*, 5348.

Slightly different values for the equilibrium constants $K(o/h)$ in Ar (0.45) and in N_2 (0.22) matrices reported previously²⁸ were based on less well-resolved spectra. We believe the differences between the earlier report²⁸ and the present study provide some estimate of the experimental error in our estimates of this constant. ($\Delta K_1(o/h) \cong \pm 0.15$ for the Ar matrix and about ± 0.30 for the N_2 matrix.)

The conclusion that both tautomers of cytosine exist in both argon and nitrogen matrices and that the a-h tautomer is present in higher concentrations is indisputable, and it is in sharp contrast with findings about these tautomeric equilibria in solutions and in the solid state, where the a-o tautomer is found predominantly.²⁹⁻³⁶

No absorption that could be assigned to the stretching vibration of an NH imino group (C=NH) for the imino tautomeric form of cytosine was found in the matrix-sample spectrum. This absorption, expected near 3320 cm^{-1} ,^{13,25,65,66} is usually very weak (about 8 times weaker than the NH stretching mode of the NH_2 group in ordinary amines⁶⁷). It seems, however, that a small concentration of cytosine molecules in the imino-oxo form may possibly be present in an Ar matrix sample, as indicated by weak absorption near 3498 cm^{-1} (corresponding possibly to the N1H stretching mode). From the ratio of the integrated absorbance of the band near 3498 cm^{-1} to that corresponding to the OH stretch of the a-h form and to that of the N1H stretch related to the a-o form in Ar matrix, the equilibrium constant for the imino form in equilibrium with the a-h form is estimated to be $K_1(i/a-h) \leq 0.05$ and, for the equilibrium with (a-o) form, $K_1(i/a-o) \leq 0.1$.

2. Vibrational Assignment. The vibrational assignment of the experimental spectrum of cytosine isolated in Ar and N_2 matrices to the normal modes predicted by the calculations for a-o and a-h tautomeric forms is given in Table I. Although the assignment is much easier after experimental separation of the spectra of the a-o and a-h tautomer resulting from the UV irradiation procedure and computer subtraction to obtain the spectra of a-o and a-h tautomers, it is still not straightforward. This is due to the effect on the spectra of such factors as discussed below.

The first complication is the presence in the matrix of more than one type of a-h tautomer (possibly different rotamers), clearly indicated by the splitting of the bands in Figure 1a bands 1439 and 1428 cm^{-1} (Figure 2, parts 1 and 2, spectrum a) as well as in splitting of other weaker bands (see Table III and Figure 2, parts 2 and 3, spectrum a). Study of the effect of UV irradiation on the relative intensities of the components of the split bands in the spectrum of the a-h tautomer indicates that the ratio depends on the duration of the UV irradiation. This effect is clearly visualized in spectrum b in Figures 1 and 2 where the bands related to the second hydroxy form appear as negative absorbances. More detailed results and discussion of the effect of UV irradiation on the spectrum of cytosine isolated in an argon matrix will be given elsewhere.⁶⁸

The second complication is the possible presence in the matrix of a small concentration of cytosine molecules in the imino-oxo tautomeric form, which may cause the appearance of weak bands that can be related to this tautomer (see Table III). The approximate positions of these bands may be expected at frequencies close to those observed for matrix-isolated 3-methylcytosine, which was found to exist in the matrix predominantly in the imino-oxo form.^{13,25,28}

A third complication in the interpretation is expected from splitting of some bands from anharmonicity effects (Fermi resonance and anharmonic coupling of normal modes). Fermi resonance is most certainly responsible for the multicomponent absorption observed in the carbonyl region of the spectrum for the a-o tautomer (see Table III and Figure 1, spectrum a and b).

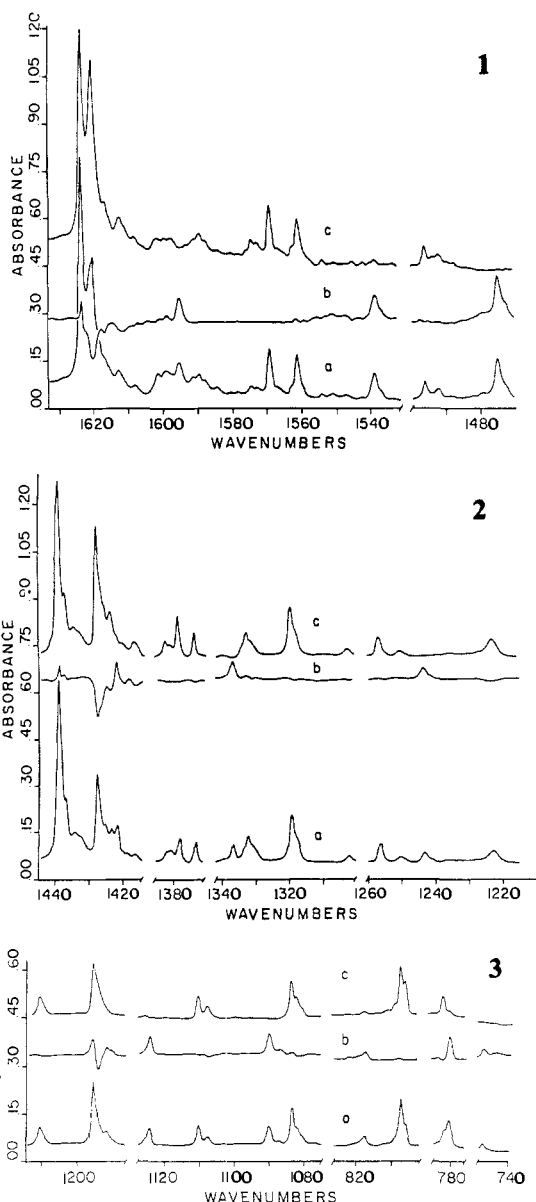


Figure 2. Infrared spectrum of cytosine isolated in an argon matrix at 15 K: spectral region $1630\text{--}1470\text{ cm}^{-1}$ (part 1); spectral region $1440\text{--}1220\text{ cm}^{-1}$ (part 2); spectral region $1210\text{--}740\text{ cm}^{-1}$ (part 3). Description of a-c is the same as in Figure 1. Region below 740 cm^{-1} listed in Tables I and III.

A fourth complication may occur because of the presence in the matrix of traces of associated molecules, which may also be responsible for the appearance of weak bands. However, the concentration of associated molecules must be very small, as indicated by the absence of significant absorption in the region of the hydrogen-bonded NH group ($3200\text{--}2800\text{ cm}^{-1}$).

Finally, splitting of some bands into two (or more) components separated by a few wavenumbers may result from matrix effects (e.g. different trapping sites) and/or the possible presence of N_2 and other impurities.

All the factors mentioned above may lead to the appearance in the experimental spectrum of cytosine of several components for each band instead of a single structureless band predicted by the calculation.

In spite of all effects discussed above, which complicate the interpretation of the spectrum of matrix-isolated cytosine, the experimental frequencies of the assigned bands are close to the calculated (scaled) frequencies, even with only a single scaling factor (0.91) for all normal modes. For most of the in-plane normal modes the differences between calculated (scaled) and experimental frequencies are of the order of a few wavenumbers.

(65) Mason, S. F. *J. Chem. Soc.* **1959**, 1281.

(66) Dreyfus, M.; Dodin, G.; Bensaude, O.; Dubois, J. E. *J. Am. Chem. Soc.* **1977**, *99*, 7027.

(67) KuBulat, K., unpublished calculations from this laboratory.

(68) Szczesniak, M.; Person, W. B.; Szczepaniak, K. to be published.

Table I. Wavenumbers, $\bar{\nu}$, Integrated Intensities, A , and Potential Energy Distributions, PEDs, for Amino-Oxo and Amino-Hydroxy Tautomers of Cytosine Monomers

normal coordn no.	calcn			experiment (Ar) ^a		normal coordn no.	calcn			experiment (Ar) ^a	
	$\bar{\nu},^b$ cm ⁻¹	A , km/mol	PED ^g	$\bar{\nu},^c$ cm ⁻¹	A^d		$\bar{\nu},^b$ cm ⁻¹	A , km/mol	PED ^g	$\bar{\nu},^c$ cm ⁻¹	A^d
Amino-Oxo Tautomer											
1	3562	67	N8H9 str (39) N8H10 str (61)	3565	81	19	891	4	N1C2 str (31) C4C5 str (25)		
2	3466	105	N1H str (100)	3471	143				NH2 rock (13)		
3	3442	105	N8H9 str (61) N8H10 str (39)	3441	209	20	882	319	C=O oopl wag (24) C4N8 oopl wag (32)	781	41
4	3123	2	C5H str (91)						C5H oopl wag (15)		
5	3086	3	C6H str (91)						OOP ring def 1 (18)		
6	1773	682	CO str (71)	1720	872	21	861	12	N1H oopl wag (20)	818	14
7	1663	590	N3C4 str (16) C5C6 str (41) C6H bend (12)	1656	424				C=O oopl wag (44) C5H oopl wag (29)		
8	1642	117	NH2 sciss (93)	1595	71	22	765	5	C4N8 oopl wag (23)	623	6
9	1544	271	N3C4 str (33) N1H bend (21)	1539	97				C5H oopl wag (32) oopl ring def 1 (16)		
10	1482	131	N1C6 str (11) C4N8 str (13) C5H bend (29) C6H bend (24)	1475	189	23	743	3	N1C2 str (24) C2N3 str (10) C4C5 str (24) C4N8 str (11)	747	5
11	1420	124	N3C4 str (10) C4C5 str (11) N1H bend (43)	1422	56	24	692	140	N1H oopl wag (73) C=O oopl wag (10)	637	8
12	1354	148	C4N8 str (29) C5H bend (13) C6H bend (17)	1337	46	25	598	139	N8H9 tors (82)	614	40
13	1236	77	C2N3 str (13) N1H bend (10) C5H bend (18) C6H bend (33)	1244	36	26	582	3	ring def 3 (75)	575	6
14	1205	22	C2N3 str (26) C4N8 str (13)	1192	70	27	535	5	C4N8 str (12)	537	6
15	1107	7	C5C6 str (10) N1C6 str (42) C5H bend (23)	1124	36	28	525	5	ring def 2 (74) CO bend (53)	532 ^e	5
16	1078	12	C5H oopl wag (25) C6H oopl wag (87)	1087	8	29	452	177	C4N8 bend (19) oopl ring def 3 (22) N8H10 tors (62)	330	30
17	1072	81	N1C2 str (14) CO bend (15) NH2 rock (39)	1090	53	30	442	9	C4N8 oopl wag (10) oopl ring def 1 (14) oopl ring def 3 (28)	409 ^e	20
18	972	0	C4C5 str (15) ring def 1 (62)			31	354	4	N8H10 tors (37) CO bend (15)	360 ^e	8
Amino-Hydroxy Tautomer											
1	3563	67	N8H9 str (41) N8H10 str (59)	3565	105	12	1314	193	CO str (13) OH bend (13)	1320	111
2	3553	119	OH str (100)	3591	182				C6H bend (36)		
3	3446	101	N8H9 str (59) N8H10 str (41)	3445	132	13	1238	199	OH bend (45)	1257	16
4	3110	5	C5H str (89) C6H str (11)			14	1155	3	NH2 rock (10) N1C2 str (20)	1193	126
5	3079	16	C5H str (11) C6H str (89)						C2N3 str (18) N3C4 str (14) N1C6 str (23)		
6	1648	174	NH2 sciss (94)	1600	63				NH2 rock (13)		
7	1602	479	C2N3 str (21) C5C6 str (27) C6H bend (11)	1623	597	15	1126	29	C5C6 str (27) C5H bend (29)	1110	29
8	1550	365	N1C2 str (15) C4C5 str (26) N1C6 str (13)	1569	179	16	1088	4	C5H oopl wag (22) C6H oopl wag (89)		
9	1530	17	C2N3 str (14) N3C4 str (13) CO str (15) C4N8 str (11) ring def 1 (12) C5H bend (10)	1496	26	17	1063	114	N3C4 str (21) N1C6 str (15)	1084	50
10	1462	400	N1C2 str (20) CO str (13) C5H bend (13) C6H bend (32)	1439	581	18	974	10	OH bend (13) NH2 rock (26) C4C5 str (18)	980	10
11	1389	59	C5C6 str (15) C4N8 str (24) ring def 1 (12) C5H bend (21)	1379	74	19	954	24	ring def 1 (48) N1C2 str (29) C4C5 str (18)	955	6
						20	911	230	NH2 rock (16) C4N8 oopl wag (32) C6H oopl wag (37) C6H oopl wag (10) oopl ring def 1 (15)	807	58
						21	846	19	CO oopl wag (29) C5H oopl wag (29) oopl ring def 1 (41)	717	16

Table I (Continued)

normal coordn no.	calcn			experiment (Ar) ^a		normal coordn no.	calcn			experiment (Ar) ^a	
	$\bar{\nu}$, ^b cm ⁻¹	A, km/mol	PED ^g	$\bar{\nu}$, ^c cm ⁻¹	A ^d		$\bar{\nu}$, ^b cm ⁻¹	A, km/mol	PED ^g	$\bar{\nu}$, ^c cm ⁻¹	A ^d
22	779	12	C4C5 str (24) CO str (10) C4N8 str (12) ring def 1 (11) ring def 3 (16)	782	16	28	484	5	CO bend (55) C4N8 bend (32)		
						29	482	55	C4N8 oopl wag (11) N8H9 tors (11) oopl ring def 1 (11) oopl ring def 3 (47)	451 ^e	6
23	762	0	CO oopl wag (30) C4N8 oopl wag (37) C5H oopl wag (14) oopl ring def 2 (11)	751	2	30	462	147	N8H10 tors (97)	297 ^e	35
						31	332	14	CO bend (28) C4N8 bend (50)	350 ^e	8
24	597	0	CO str (21) ring def 3 (63)	601	10	32	233	17	CO oopl wag (16) C4N8 oopl wag (14)		
25	571	259	N8H9 tors (79) oopl ring def 1 (10)	520	66				oopl ring def 1 (26) oopl ring def 3 (35)		
26	564	4	C4N8 str (12) ring def 2 (76)	569	6	33	214	0	oopl ring def 2 (78) oopl ring def 3 (15)		
27	518	93	OH oopl wag (93)	507	37						

^aDilute in argon matrix at 15 K. ^bWavenumbers scaled by a constant factor of 0.91. ^cOnly the strongest band is given when multicomponent bands are observed. All bands observed are listed in Table III. ^dIntegrated relative intensities in the unit chosen in such a way that the observed intensity sum of the in-plane modes observed in the separated spectra of a-o or a-h tautomer is equal the calculated intensity sum of these modes. The experimental intensities correspond to all components of multicomponent bands if splitting is observed. ^eFor cytosine in the N₂ matrix.²⁵ ^fBelow the region studied experimentally. Wavenumbers for crystalline solid are from ref 69. ^gAbbreviations: str, stretching; bend, bending; sciss, scissors; oopl, out of plane; wag, wagging; rock, rocking; def, deformation; tors, torsion.

Larger differences are found for C=O and C=C in-plane stretching vibrations, but the assignment for these vibrations is quite obvious. As is usual for calculations at this level, a larger discrepancy is observed between the calculated (scaled) and experimental frequencies for the out-of-plane modes. Hence, the assignment of these latter modes is still *very* uncertain.

The calculated intensity patterns agree with the experimentally observed patterns within the usual^{19b} "factor of about 2" with a few exceptions for weak bands and out-of-plane modes. It has to be mentioned that the experimental intensities given in Table I correspond to the intensities of the bands in the spectrum of a-h and a-o tautomers as separated after performing the subtraction procedure. This procedure may also introduce some error in the experimental estimates of relative integrated intensities of the bands.

The experimental spectrum was studied in the spectral region down to 250 cm⁻¹. Below this region two more normal modes are predicted for both tautomers. The frequencies of these modes predicted for the a-o tautomer are close to those observed experimentally for crystalline cytosine at 232 and 197 cm⁻¹.⁶⁹

The spectrum of *D*-cytosine was analyzed in a similar way as was the spectrum of cytosine. The resulting assignment is given in Table II for each tautomer. In the assignment of the absorption bands from *D*-cytosine to the calculated normal modes, a comparison of its experimental spectrum with that of cytosine (see Figure 3) was also very helpful. In particular, it allows us to check the assignment of the bands related to the vibrations of the NH, ND and NH₂, ND₂ groups.

Calculations were performed also for all isotopically substituted cytosines. The results can be obtained upon request. The experimental spectra have not yet been studied.

When our results are compared with those of other authors,^{15,37} it is important to emphasize that all studies agree on the conclusions about the presence in matrix of both a-o and a-h tautomers. There is also general agreement between spectra from all studies. On close examination we found small differences in frequencies, with larger differences in relative intensities and splittings of the bands. Some of these frequency differences probably result from differences in the calibration of the spectrometers, but general differences in the spectra also result from less trivial reasons, such as the different resolution of the spectrometers, different conditions of the preparation of the matrix, and, particularly, different temperatures of the cold window. It is known that details in the appearance of matrix spectra from

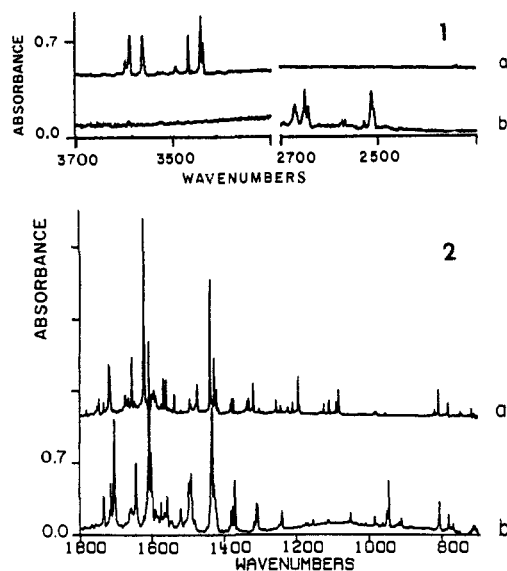


Figure 3. Infrared spectrum in the 3700–2500-cm⁻¹ region (part 1) and 1800–700-cm⁻¹ region (part 2) of (a) cytosine and (b) *D*-cytosine both isolated in an Ar matrix. Region below 740 cm⁻¹ listed in Tables I–III.

different experiments are very sensitive to these factors.

Our assignment (and also that by Nowak³⁷) of the bands to the a-o and a-h tautomers and to the normal modes differs in many cases from that by Radchenko et al.,¹⁵ who were not able to separate experimentally the spectra of the two tautomeric forms. The most drastic difference between the two assignments is that concerning the scissors vibration of the NH₂ group. Radchenko et al. assigned the band at 1749 cm⁻¹ to the NH₂ scissors vibration of the a-o tautomer and that at 1670 cm⁻¹ to the NH₂ scissors mode of the a-h tautomer, taking into account changes in this region upon deuteration. Such a drastic difference between the NH₂ groups measured by the frequencies of this vibration for the NH₂ group in the a-o form compared with that in the hydroxy tautomer seems rather unlikely, since the frequencies for the stretching vibrations are so close together for the NH₂ group in each of the two tautomeric forms, in fact so close that they were not distinguished in the spectrum reported by those authors. It seems more likely that the absorption near 1749 cm⁻¹ observed by Radchenko et al.¹⁵ for cytosine (which contains several components visible under the higher resolution of our study; see Table III) is due Fermi resonance between the C=O stretch and a

Table II. Wavenumbers, $\bar{\nu}$, Integrated Intensities, A , and Potential Energy Distributions, PEDs, for Amino-Oxo and Amino-Hydroxy Tautomers of Deuteriated Cytosine Monomers (Calculated Results for Deuteriated Tautomers at Amino Group and N₁ or O atoms)

normal coordin no.	calcn			experiment		normal coordin no.	calcn			experiment	
	$\bar{\nu},^b$ cm ⁻¹	A , km/mol	PED ^f	$\bar{\nu},^c$ cm ⁻¹	A^d		$\bar{\nu},^c$ cm ⁻¹	A , km/mol	PED ^f	$\bar{\nu},^c$ cm ⁻¹	A^d
Amino-Oxo Tautomer											
1	3123	2	C5H str (91)			18	927	3	ring def I (22)	923	6
2	3087	3	C6H str (91)						N1D bend (27)		
3	2640	39	N8D9 str (43)	2672	49				ND2 rock (15)		
			N8D10 str (57)			19	880	256	C=O oopl wag (19)	782	63
4	2543	77	N1D str (98)	2573	74				C4N8 oopl wag (35)		
5	2486	90	N8D9 str (56)	2510	93				C5H oopl wag (19)		
			N8D10 str (42)						oopl ring def 1 (18)		
6	1762	691	CO str (76)	1706	744	20	851	6	C=O oopl wag (53)		
7	1655	485	N3C4 str (18)	1645	490				C5H oopl wag (28)		
			C5C6 str (43)			21	796	2	N1C2 str (11)	775	6
			C6H bend (11)						C4C5 str (22)		
8	1513	376	N3C4 str (44)	1492	205				ND2 rock (42)		
			C5C6 str (18)			22	753	2	C=O oopl wag (15)		
9	1480	147	C4C5 str (13)	1495	161				C4N8 oopl wag (30)		
			N1C6 str (11)						C5H oopl wag (29)		
			C4N8 str (13)						oopl ring def 1 (13)		
			C5H bend (31)						oopl ring def 2 (11)		
			C6H bend (23)			23	733	2	N1C2 str (25)	751	6
10	1360	266	C4N8 str (35)	1371	180				C4C5 str (22)		
			C5H bend (11)						C4N8 str (10)		
			C6H bend (13)			24	579	3	ring def 3 (72)	485	2
			ND2 sciss (10)			25	530	98	N1D oopl wag (95)	430	10
11	1304	97	N1C6 str (30)	1318	81	26	516	5	C4N8 str (15)	520	6
			N1D bend (16)						ring def 2 (68)		
			C6H bend (23)			27	500	5	CO bend (57)	508	6
12	1230	16	C2N3 str (22)	1195	3				C4N8 bend (11)		
			ND2 sciss (38)			28	495	29	oopl ring def 1 (20)	408	6
13	1178	20	N1D bend (11)	1174	3				oopl ring def 2 (12)		
			C5H bend (38)						oopl ring def 3 (20)		
			C6H bend (18)						N8D9 tors (43)		
14	1154	26	C2N3 str (20)	1155	19	29	408	98	C4N8 oopl wag (11)	<i>e</i>	
			ND2 sciss (40)						oopl ring def 3 (34)		
15	1077	7	C5H oopl wag (26)			30	332	41	N8D9 tors (47)	<i>e</i>	
			C6H oopl wag (88)			31	320	3	N8D10 tors (92)	<i>e</i>	
16	988	18	N1C2 str (20)						C4N8 bend (62)	<i>e</i>	
			C4C5 str (13)						ND2 rock (11)		
			ring def 1 (28)			32	207	16	oopl ring def 1 (33)	<i>e</i>	
			CO bend (10)						oopl ring def 3 (42)		
			ND2 rock (11)			33	161	6	oopl ring def 2 (86)	<i>e</i>	
17	961	24	N1C6 str (23)	964	12				oopl ring def 3 (14)		
			ring def 1 (13)								
			N1D bend (29)								
Amino-Hydroxy Tautomer											
1	3110	5	C5H str (89)			10	1387	172	C5C6 str (14)	1378	122
			C6H str (11)						C4N8 str (23)		
2	3079	15	C5H str (11)						C5H bend (26)		
			C6H str (89)			11	1308	63	N1C6 str (13)	1309	112
3	2640	37	N8D9 str (44)	2670	40				CO str (16)		
			N8D10 str (55)						C6H bend (39)		
4	2586	72	OD str (100)	3651	88	12	1204	20	ND2 sciss (75)	1243	37
5	2489	91	N8D9 str (55)	2515	75	13	1149	75	N1C2 str (16)	1176	8
			N8D10 str (44)						C2N3 str (11)		
6	1594	557	C2N3 str (17)	1609	572				N3C4 str (11)		
			N3C4 str (10)						C4C5 str (12)		
			C5C6 str (30)						C5C6 str (24)		
			C6H bend (12)						N1C6 str (11)		
7	1543	388	N1C2 str (12)	1568	102	14	1126	7	N3C4 str (13)	1115	8
			C4C5 str (22)						C5C6 str (12)		
			N1C6 str (13)						N1C6 str (24)		
			C4N8 str (10)						C5H bend (34)		
			C5H bend (12)			15	1088	4	C5H oopl wag (22)	1052	18
8	1510	1	C2N3 str (19)	1499	78				C6H oopl wag (89)		
			N3C4 str (20)			16	1033	2	CO str (13)	1034	3
			CO str (11)						C4N8 str (12)		
			C4N8 str (12)						OD bend (12)		
			ring def 1 (12)						ND2 rock (10)		
9	1462	443	N1C2 str (20)	1434	373	17	972	18	N1C6 str (10)	913	20
			CO str (14)						ring def 1 (51)		
			C5H bend (13)			18	923	156	N1C2 str (19)	947	88
			C6H bend (30)						OD bend (59)		

Table II (Continued)

normal coordn no.	calcn			experiment (Ar) ^a		normal coordn no.	calcn			experiment (Ar) ^a	
	$\bar{\nu},^b$ cm ⁻¹	A, km/mol	PED ^f	$\bar{\nu},^c$ cm ⁻¹	A ^d		$\bar{\nu},^b$ cm ⁻¹	A, km/mol	PED ^f	$\bar{\nu},^c$ cm ⁻¹	A ^d
19	910	202	C4N8 oopl wag (32) C5H oopl wag (38) C6H oopl wag (10) oopl ring def 1 (15)	809	55	26	508	26	CO oopl wag (11) N8D9 tors (13) oopl ring def 1 (21) oopl ring def 2 (12) oopl ring def 3 (38)	406	10
20	845	13	CO oopl wag (30) C5H oopl wag (28) oopl ring def 1 (42)	748	3	27	441	8	CO bend (56) C4N8 bend (23)	451	6
21	837	3	C4C5 str (17) ND2 rock (59)	838	3	28	412	184	N8D9 tors (70) oopl ring def 3 (18)	e	
22	762	11	C4C5 str (22) C4N8 str (11) ring def 3 (21)	770	8	29	386	66	OD oopl wag (92)	e	
23	757	1	CO oopl wag (31) C4N8 oopl wag (39) C5H oopl wag (15) oopl ring def 2 (11)	749	4	30	343	17	N8D10 tors (84)	e	
24	587	0	CO str (21) ring def 3 (57)	595	2	31	299	11	CO bend (22) C4N8 bend (53)	e	
25	548	3	C4N8 str (15) ring def 2 (70)			32	217	27	CO oopl wag (20) oopl ring def 1 (20) oopl ring def 2 (26) oopl ring def 3 (17)	e	
						33	209	5	C4N8 oopl wag (11) oopl ring def 2 (57) oopl ring def 3 (28)	e	

^{a-d}The same as in Table I. ^eBelow the region studied experimentally. The same as g in Table I.

combination of lower frequency modes. A similar Fermi resonance splitting of the carbonyl stretching absorption into several components has been observed for uracils isolated in low-temperature matrices.^{19,21,22,24} These latter studies indicate also that the infrared spectral pattern observed in the carbonyl stretching region depends strongly on the deuteration of the ring nitrogen atoms of uracils, probably because of the effect of deuteration on the low-frequency combination modes and, hence, on the Fermi resonance pattern. A weak band near 1750 cm⁻¹ observed for the a-h tautomer of cytosine might be assigned to a combination vibration (e.g. 1439 + 332 or 1193 + 569). No absorption is present in the spectrum of the a-h form (Figure 1, spectrum c) near 1670 cm⁻¹, and this rules out the assignment of Radchenko et al.¹⁵ for the band at this frequency to the NH₂ scissors vibration of the a-h tautomer.

We have assigned a weak band near 1600 cm⁻¹ to the NH₂ scissors vibration for cytosine. This absorption clearly contains several components, which could be due to the different NH₂ groups from the a-o and a-h tautomers. No absorption near 1600 cm⁻¹ is observed in the spectrum of matrix-isolated *D*-cytosine (see Figure 3). A relatively strong absorption near 1600 cm⁻¹ was also observed in the spectrum of 1-methylcytosine isolated in inert matrices^{25,44} but not in its deuterated analogue. An additional support for choosing the absorption near 1600 cm⁻¹ to be the NH₂ scissors in preference to that near 1749 cm⁻¹ is obtained from matrix-isolation studies of 2-amino-5-chloropyrimidine, for which no significant absorption is recorded in the region above 1630 cm⁻¹ but relatively strong bands are observed near 1600 cm⁻¹.^{16,25}

We believe that our assignment of the observed bands to the a-o and a-h tautomers and to the normal modes should be quite reliable because it is based on the experimentally separated spectra of these tautomers resulting from the UV irradiation procedure and because it makes use of a more reliable SCF-MO ab initio calculation of frequencies and intensities for the normal modes.

According to our knowledge, the only previous ab initio calculation of the infrared spectrum of cytosine is that of Nishimura and Tsuboi using an STO-3G basis set.³⁹ In this calculation only the amino-oxo form was considered, and only frequencies (but not intensities) for the in-plane normal modes have been calculated. The frequencies obtained by these authors (which we scaled additionally by the same single scaling factor (0.91) as for the frequencies from our calculations, for comparison purposes, to bring them in better agreement with experimental frequencies) agree quite well with those predicted by our calculation for the amino-oxo tautomer. The main discrepancy between the two calculations concerns the contributions (the PEDs)⁷⁰ of internal

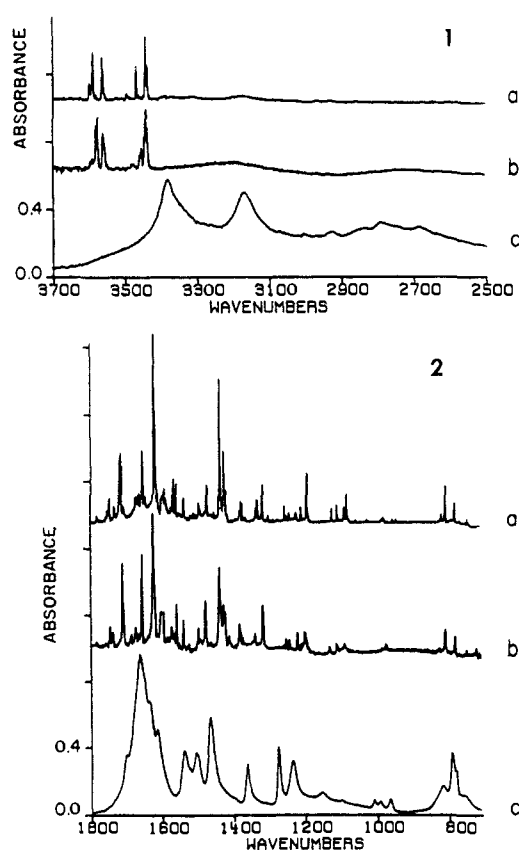


Figure 4. Infrared spectrum in the 3700–2500-cm⁻¹ region (part 1) and 1800–700-cm⁻¹ region (part 2) of cytosine (a) in Ar matrix, (b) in N₂ matrix, and (c) as a crystalline solid in KBr. Region below 740 cm⁻¹ listed in Table III.

coordinates to the normal modes located in the region 1000–1700 cm⁻¹. In this region mainly ring stretching modes, together with several in-plane bending modes, are located. It is known that these normal modes are usually strongly coupled and that PEDs strongly depend upon the interactions of force constants.

3. Effect of Intermolecular Interactions on Tautomerism and on the IR Spectrum of Cytosine. The effect of intermolecular interactions on the tautomeric equilibrium and on the IR spectrum of cytosine was studied by comparing the spectrum of cytosine isolated in an inert Ar matrix with the spectrum of cytosine first isolated in the slightly more active N₂ matrix and then surrounded

(70) (a) Morino, Y.; Kuchitsu, K. *J. Chem. Phys.* **1952**, *20*, 1809. (b) Keresztury, G.; Jalsovsky, G. *J. Mol. Struct.* **1971**, *10*, 304.

Table III. Experimental Wavenumbers, $\bar{\nu}$, Integrated Absorbance, I , Assignment of Bands in the Spectrum of Cytosine in the Ar and N₂ Matrices and in Crystalline Solid, and N-Deuteriated Cytosine in the Ar Matrix^{a-c}

cytosine										
Ar			N ₂			solid in KBr		N-deuteriated cytosine: Ar		
$\bar{\nu}$, cm ⁻¹	I	assign	$\bar{\nu}$, cm ⁻¹	I	assign	$\bar{\nu}$, cm ⁻¹	assign	$\bar{\nu}$, cm ⁻¹	I	assign
3601	22	H	3598					2672	153	H,O; Q ₃
3591	93	H; Q ₂	3592					2657	31	
			3581					2651	213	H; Q ₃
			3577	119	H; Q ₂			2622	6	
3565	94	H, O; Q ₁	3562	81	H, O; Q ₁	3380	O; Q ₁	2578	25	O; Q ₄
3563			3556			2925		2573	49	
3498	6	I-N1H?				2850		2554	18	
3471	41	O; Q ₂	3460	39	O; Q ₂	2800	O; Q ₂	2530	30	
3451	2	I-N3H?	3456			2780		2525		
3445	96	H; Q ₃	3447			2675		2515	177	H; Q ₃
			3443	90	H; Q ₃			2510	93	O; Q ₃
3441	63	O; Q ₃	3440			3170				
			3439	52	O; Q ₃					
1782	4	O; FR								
1753	10	O; FR								
1750	10	H; Comb						1737	213	H; Comb
1747	26	O; FR	1747	21	O; FR			1715	207	O; FR
1734	12	O; FR	1738	17	O; FR			1713		
1720			1712	123	O; Q ₆	1662	O; Q ₆	1706	421	O; Q ₆
1717	195	O; Q ₆								
1675	20	I-?	1675	15	I-?					
1671										
1666	16	I-?								
1656	89	O; Q ₇	1657	76	O; Q ₇	1640	O; Q ₇	1659	110	
1648	16	O				1613		1645	372	O; Q ₇
1623	365	H; Q ₇	1626	244	H; Q ₇					
1620		H								
1612		H						1609	946	H; Q ₆
1600		H; Q ₆	1604	68	H; Q ₆			1603	421	H
1595	123	O; Q ₈	1601		O; Q ₈	1700	O; Q ₈	1589	30	H
1590		H	1585	7	H					H
			1578	4	H					H
1575	3	H	1574	20	H			1577	60	H
1573										
1569	32	H; Q ₈	1565	7	H; Q ₈			1568	97	H; Q ₇
1561	34	H	1560	24	H			1559	60	H
1539	25	O; Q ₉	1541	18	O; Q ₉	1540	O; Q ₉	1522	66	H
1496	12	H; Q ₉	1498	12	H; Q ₉			1499	110	H; Q ₈
1492	8	I-?						1497	79	H
1475	50	O; Q ₁₀	1479	40	O; Q ₁₀	1505	O; Q ₁₀	1495	159	O; Q ₉
1439	229	H; Q ₁₀	1440	153	H; Q ₁₀			1492	201	O; Q ₈
1434		H						1441	49	O
1428	159	H	1429	51	H			1438	171	H
1424		H						1434	738	H; Q ₉
1422		O; Q ₁₁	1425	31	O; Q ₁₁	1463	O; Q ₁₁	1428	348	H
1416	5	H	1413	4	H			1422	256	H
1382	11	H						1389	18	H
1379	12	H; Q ₁₀	1385	30	H; Q ₁₁			1383	110	H
1374	10	H	1374	4	H			1378	171	H; Q ₁₀
1337	7	O; Q ₁₂	1341	5	O; Q ₁₂	1363	O; Q ₁₂	1371	177	O; Q ₁₀
1333	29	H						1342	6	H
1320	42	H; Q ₁₂	1319	50	H; Q ₁₂			1318	79	O; Q ₁₁
1303	8							1316		H
1257	15	H	1254	8	H			1312		
1250	5	H						1309	274	H; Q ₁₁
1244	9	O; Q ₁₃	1245	7	O	1278	O; Q ₁₃	1250		H
1223	17	H	1222	18	H			1243	366	H; Q ₁₂
1210	15	H	1212		H			1240		H
1195	63	H; Q ₁₄	1207		H; Q ₁₄			1195	3	O; Q ₁₂
1192		O; Q ₁₄	1202	53	O; Q ₁₄	1238	O; Q ₁₄	1176	16	H; Q ₁₃
1124	11	O; Q ₁₅	1199		O	1100	O; Q ₁₅	1174	6	O; Q ₁₃
1110	11	H; Q ₁₅	1196		O			1170	6	H
1108	5	I-?	1134	9	O; Q ₁₅					
1090	13	O; Q ₁₇	1132			1150	O; Q ₁₇	1155	18	O; Q ₁₄
1087	2	O; Q ₁₆								
1084	32	H; Q ₁₇	1114	10	H; Q ₁₅			1115	18	H; Q ₁₄
1082		H	1110		O; Q ₁₆			1052	42	H; Q ₁₅
980	9	H; Q ₁₈	1091	6	H; Q ₁₆			1034	6	H; Q ₁₆
955	2	H; Q ₁₉	975	6	H; Q ₁₈			1010	12	H
818	9	O; Q ₂₁				1010	O; Q ₁₈	1007		H
807	36	H; Q ₂₀	810	25	H; Q ₂₀	996	O; Q ₁₆	986	25	H
782	25	H; Q ₂₂	783	18	H; Q ₂₂	966	O; Q ₁₉	972		O
						885				

Table III (Continued)

cytosine											
Ar			N ₂			solid in KBr		N-deuteriated cytosine: Ar			
$\bar{\nu}$, cm ⁻¹	<i>I</i>	assign	$\bar{\nu}$, cm ⁻¹	<i>I</i>	assign	$\bar{\nu}$, cm ⁻¹	assign	$\bar{\nu}$, cm ⁻¹	<i>I</i>	assign	
781		O; Q ₂₀				820	O; Q ₂₁	964	12	O; Q ₁₇	
751	2	H; Q ₂₃	752	5	H; Q ₂₃	791	O; Q ₂₀	959	6	H	
747	4	O; Q ₂₃	726	8	O; Q ₂₁	780	O; Q ₂₃	953	6		
717	14	O; Q ₂₁	716	5	O; Q ₂₃	760	O; Q ₂₄	947	201	H; Q ₁₈	
710	8	H				700	O; Q ₂₅	923	6	Q; Q ₁₈	
637	14	O; Q ₂₄	643	20	O; Q ₂₄			918	6	H	
623	6	O; Q ₂₂						913	49	H; Q ₁₇	
614	24	O; Q ₂₅						885	6	O	
601	20	H; Q ₂₄				600	O; Q ₂₆	838	6	H; Q ₂₁	
595	4	H									
575	14	O; Q ₂₆									
569	6	H; Q ₂₆	555	53	H; Q ₂₇			809	134	H; Q ₁₉	
559	12	H				565		782	61	O; Q ₁₉	
555	2	H				545	O; Q ₂₈	775	6	O; Q ₂₁	
								770	31	H; Q ₂₂	
537	6	O; Q ₂₇	537	6	O; O ₂₇	530	O; Q ₂₇	751	5	O; Q ₂₃	
532	5	O; Q ₂₈	532	5	O; O ₂₈			748	5	H; Q ₂₃	
520	66	H; Q ₂₅	513	10	H; Q ₂₅			595	6	H; Q ₂₄	
507	37	H; Q ₂₇	507	37	H; Q ₂₇	500	O; Q ₂₉				
			451	6	H; Q ₂₉	440	O; Q ₃₀				
			409	5	O; Q ₃₀	425	O; Q ₃₁				
			360	8	O; Q ₃₁						
			350	8	H; Q ₃₁						
			330	30	O; Q ₂₉						
			297	35	H; Q ₃₀						

^aWavenumbers of the most intense bands are italicized. ^bIntegrated intensities are expressed in relative arbitrary units. Data from original spectra before UV irradiation and subtraction procedures. When bands consist of several components which cannot be resolved, the total intensity of all components is given in the table next to the peak of the band (with italicized wavenumber). The error of the intensity determination for the well resolved bands is about $\pm 10\%$. For overlapped bands the error is much larger. ^cH, amino-hydroxy form; O, amino-oxo form; Q_n, normal mode according to normal coordinates in Tables I and II; *I*, possibly absorption of imino forms (see text); FR, Fermi resonance with the carbonyl or other mode; comb, combination modes.

by other cytosine molecules in the crystalline solid (Figure 4 and Table III).

It is known from the numerous studies of small molecules isolated in Ar and N₂ matrices (ref 17 and 18 and references given therein) that the interaction of trapped molecules with the N₂ matrix is significantly stronger than that with an Ar matrix and that there is a pronounced effect of this interaction on the IR spectrum of the molecule.

In the case of cytosine the spectrum from the N₂ matrix is similar to that from the Ar matrix in its general appearance (Figure 4). On close examination differences in frequencies, relative intensities and band splittings are found. These differences may be seen even in the survey spectrum shown in Figure 4, and details are listed in Table III.

As was mentioned before, the oxo \rightleftharpoons hydroxy equilibrium constant does not differ significantly when measured in Ar from the value in the N₂ matrix. There is, however, a shift to low frequency in N₂ compared to Ar matrices of the OH and N1H stretches by about 14–15 cm⁻¹, and (most probably) the molar absorption coefficient of the OH stretch increases by about 2.5 times that of $\nu(\text{N1H})$ in the N₂ matrix. Surprisingly, the shift to lower frequencies of the absorption bands related to the NH₂ stretches is only 2–3 cm⁻¹ in the N₂ matrix. The C=O stretch also shifts down by about 8 cm⁻¹ in the N₂ matrix, and the frequency shifts of most of the other bands are even smaller. The splitting of the bands into several components is in general less pronounced in the N₂ than in the Ar matrix spectra. This may be due to the fact that the width of bands in the N₂ matrix spectrum is usually larger and only one broader band is observed instead of separate components found in the Ar matrix spectrum. In the Ar matrix spectrum the width at half-maximum intensity is generally about 1–2 cm⁻¹, while for the N₂ matrix it is often 2–4 cm⁻¹ or more.

All these differences of frequencies, intensities, and widths of the absorption bands observed for the Ar and N₂ matrix spectra of cytosine reflect differences in the interaction of the cytosine molecule, in particular involving its most active functional groups

(OH, N1H, NH₂, and C=O), with an Ar or N₂ environment.

A dramatic change of the IR spectrum is observed when the cytosine molecule finds itself in an environment containing other cytosine molecules in close contact, as in the crystalline solid shown in the spectrum in Figure 4. In the crystal the molecules of cytosine are involved in strong hydrogen bonds. According to the X-ray data,⁷¹ only the a-o tautomer is present in the crystal and the proton donor and proton acceptor groups participate in hydrogen bonds. In agreement with this scheme the most dramatic changes are observed in those regions of the IR spectrum where the vibrations of the proton donor groups (N1H and NH₂) and proton acceptor groups (C=O and ring nitrogen atoms) appear. The N1H stretch in solid cytosine is shifted with respect to its position in an Ar matrix spectrum down by about 670–770 cm⁻¹ and appears as a very broad band whose maximum is difficult to determine. A smaller down-frequency shift is found for the NH₂ stretches, namely about 185 and 271 cm⁻¹ for asymmetric and symmetric stretching modes, if the spectrum of the crystalline solid is correctly assigned to these modes (see Table III and also ref 72).

It is difficult to interpret the absorption in the region 1600–1700 cm⁻¹, where the the C=O stretching mode and NH₂ bending (scissors) modes are expected. We have assigned the hydrogen-bonded C=O stretch to the strongest absorption in this region of the spectrum of the solid near 1662 cm⁻¹. In making this assignment we took into account the fact that the C=O stretching mode is the most intense mode observed for the a-o monomeric molecules in Ar and N₂ matrices and also the fact that hydrogen bonding is not expected to increase strongly the intensity of the bending mode of the NH₂ group (in contrast to the usually observed strong intensification of the intensity of the NH₂ stretching modes upon hydrogen bonding). The frequency of the C=O stretch (1662 cm⁻¹) is close to that observed for the

(71) Barker, D. L.; Marsh, R. E. *Acta Crystallogr.* **1964**, *17*, 1581.

(72) Susi, H.; Ard, J. S.; Purcell, J. M. *Spectrochim. Acta, Part A* **1973**, *A29*, 725.

hydrogen-bonded C=O group in uracils.²² The bending mode of the NH₂ group is assigned to a shoulder on the main band in the spectrum of solid, at 1640 cm⁻¹ or possibly at 1700 cm⁻¹. Frequencies of the other bands observed in the IR spectrum of cytosine as a crystalline solid, together with the assignment of these bands to the normal modes of vibration for the a-oxo tautomer, are summarized in Table III. As may be seen in this table and also in Figure 4, the frequencies of most of the lower frequency modes, with the exception of those related to the bending vibrations of the N1H and NH₂ groups, are not very strongly affected by the interactions that occur between cytosine molecules in the crystal.

Conclusions

The main conclusions from the present study are outlined as follows.

1. Ab initio molecular orbital calculations have been made with a 3-21G basis set at the SCF level for the infrared spectra (vibrational frequencies, intensities, and potential energy distributions (PEDs)) for two tautomers of cytosine (i.e., the amino-oxo and amino-hydroxy forms) and for their deuterated analogues.

2. Comparison of the calculated and experimental matrix spectra confirms the existence of both the amino-oxo and the amino-hydroxy tautomeric forms of cytosine, and of its deuterated analogue, when they are isolated in the matrices and allows us to determine the ratio of the concentrations of each form (the "equilibrium constant" for tautomerization) in Ar and N₂ matrices.

3. Furthermore, this comparison permits an initial assignment of the absorption bands in the spectrum of cytosine from each tautomer.

4. Our study has verified the effect of UV irradiation on the relative concentrations of tautomers in matrix-isolated samples of cytosine and N-deuterated cytosine that has been observed earlier by Nowak.³⁷ We have been able to utilize this effect to change the ratio of tautomers in our sample and hence to use the subtraction routine of the Nicolet spectrometer to obtain exper-

imentally separated spectra for each tautomer.

5. When frequencies and intensities from these separated spectra are compared with the calculated spectra, we have been able to assign with confidence most of the spectrum of each tautomer. The reasonable agreement between the calculated and experimental spectra leads to the conclusion that the calculated force constants and intensity parameters (APTs) for each tautomer form a reasonably good starting point for the experimental values of these parameters.

6. Finally, we have examined the drastic change of the tautomeric equilibrium toward the amino-oxo form and the change of the infrared spectrum for the strongly self-associated cytosine in the crystalline solid compared with cytosine isolated in the Ar matrix. The weaker interaction with an N₂ matrix does not change tautomeric equilibrium significantly, but it does affect the vibrational frequencies and intensities of the normal modes of each tautomer, particularly those of the N1H and OH stretching modes.

Acknowledgment. We thank Dr. M. J. Nowak (Warsaw) for his remarks concerning the UV irradiation procedure based on the yet unpublished results of matrix studies of pyrimidine bases including cytosine. This investigation was supported by NIH Research Grant No. 32988 with additional partial support provided by grants from the Polish Ministry of National Education Project No. CPBP 01.06 (J.S.K.) and No. CPBR 11.5 (M.S.).

Registry No. Cytosine (amino-oxo form), 71-30-7; cytosine (amino-hydroxy form), 66460-21-7.

Supplementary Material Available: Tables of optimized (3-21G) geometries (Table 4), symmetry coordinates for the description of vibrational modes (Table 5), diagonal elements of force constants matrix (Table 6), and atomic polar tensors and their invariants (Table 7) for cytosine tautomers and Figure 5 with definition of internal coordinates (6 pages). Ordering information is given on any current masthead page.

Experimental Evidence for the Existence of Ionized and Neutral Fluorohydroxymethylene (FCOH) in the Gas Phase[†]

Detlev Sülzle, Thomas Drewello, Ben L. M. van Baar,[†] and Helmut Schwarz*

Contribution from the Institut für Organische Chemie der Technischen Universität Berlin, Strasse des 17. Juni 135, D-1000 Berlin 12, West Germany. Received March 25, 1988

Abstract: The elusive ionic and neutral fluorohydroxymethylenes (FCOH) are accessible in the gas phase by dissociative ionization of methyl fluoroformate followed by neutralization of FCOH^{•+} with xenon. The experimental findings are supported by high-level ab initio MO calculations (MP2/6-31G**//MP2/6-31G** + ZPVE). Both FCOH and FCOH^{•+} are separated by significant barriers from their respective formyl fluoride isomers.

Although fluorohydroxymethylene (**1**) is predicted¹ by ab initio molecular orbital (MO) calculations to be prevented by a significant barrier from its isomerization to the global minimum of the [H,C,O,F] potential energy surface, i.e., formyl fluoride (**2**), all attempts failed to generate **1** as a stable species in solution. In view of the high reactivity^{2,3} of most carbenes towards addition and insertion reactions, the prospects of ever generating stable fluorohydroxymethylene⁴ in the condensed phase are indeed quite remote. In contrast, in the absence of any intermolecular reactions and because of the high barrier of the process **1** → **2** ($E_0 = 40$

kcal/mol¹), elusive **1** should be accessible by performing appropriate experiments in the gas phase. We describe here the results of a mass spectrometric investigation using the powerful method

(1) Morokuma, K.; Kato, S.; Hirao, K. *J. Chem. Phys.* **1980**, *72*, 6800.

(2) (a) Kirmse, W. *Carbene, Carbenoide und Carbenanaloge*; Verlag Chemie: Weinheim, 1969. (b) March, J. *Advanced Organic Chemistry: Reactions, Mechanisms and Structures*; Wiley: New York, 1985. (c) Wentrup, C. *Reactive Molecules*; Wiley: New York, 1984.

(3) (a) Rondan, N. G.; Houk, K. N.; Moss, R. A. *J. Am. Chem. Soc.* **1980**, *102*, 1770. (b) Ahmed, S. N.; McKee, M. L.; Shevlin, P. B. *J. Am. Chem. Soc.* **1985**, *107*, 1320.

(4) According to MO calculations using the minimal STO-3G basis set, **1** is predicted to be a singlet carbene being 23.7 kcal/mol more stable than its triplet form: Mueller, P. H.; Rondan, N. G.; Houk, K. N.; Harrison, J. F.; Hooper, D.; Willen, B. H.; Liebman, J. F. *J. Am. Chem. Soc.* **1981**, *103*, 5049.

[†] Dedicated to Professor J. H. Beynon FRS on the occasion of his 65th birthday.

*Permanent address: Organic Chemistry Department, The Free University of Amsterdam, NL-1081HV Amsterdam, The Netherlands.